

SIMULATIONS FOR PROTONS AND ELECTRONS ACCELERATION WITH THE 1 PW LASER PULSE FROM CETAL FACILITY

O. BUDRIGĂ¹, E. D'HUMIÈRES², C.M. TICOȘ³

¹Laser Department, National Institute for Laser, Plasma and Radiation Physics,
P.O. Box MG-36, 077125, Magurele, Romania, EU

E-mail: olimpia.budriga@inflpr.ro

²CELIA, Universite de Bordeaux - CNRS - CEA, 33405 Talence Cedex, France, EU

E-mail: dhumieres@celia.u-bordeaux1.fr

³Laser Department, National Institute for Laser, Plasma and Radiation Physics,
P.O. Box MG-36, 077125, Magurele, Romania, EU

E-mail: catalin.ticos@inflpr.ro

Received October 4, 2015

Abstract. The new laser with a peak power of 1 PW from the CETAL facility, I.N.F.L.P.R., Romania, in the interaction with gaseous or solid targets can accelerate the electrons or protons at kinetic energies of GeV and, respectively tens of MeV. Prospective, we do particle-in-cell simulations to investigate the optimal parameters of both ultrashort laser pulse and target. We obtain for a Helium gas target that the electrons can be accelerated at the energies of 940 MeV, and for a cone and a high dense gas targets the protons can be accelerated at the energies of 70 MeV.

Key words: ultra-high power laser, laser-plasma acceleration of electrons and ions, Particle-in-Cell simulations.

1. INTRODUCTION

Laser plasma accelerators have seen an unprecedented development in the last decade attaining particle energies which once seemed a dream. This was possible by the continuous developments of the laser technology, particularly in obtaining ever shorter laser pulses with increased energy, by the refinement of the experimental methods for taking advantage of the enormous electric fields of the laser pulses and also due to seminal work by Tajima and Dawson who proposed the use of plasma waves as accelerating structures for charged particles [1]. Since then electron beams with record energies of above 1 GeV have been measured in capillary discharges [2], or in specially designed gas cells [3, 4] and proton and ion energies of the order of 100 MeV [5]. An important role in understanding the acceleration mechanism is played by the Particle-in-Cell (PIC) simulations of the laser-target interaction. In fact, the

laser-wakefield acceleration of electrons with monoenergetic energies in the plasma created by a high power laser known as the bubble regime has been first discovered numerically [6] and then validated experimentally. The protons can be accelerated at energies in the range of tens of MeV from foil and cone targets which interact with the ultra-high power and ultra-short laser pulse [7–10].

The newly built CETAL center comprises as the main facility a state-of-the-art 1 Petawatt laser system. Built on Ti-Sapphire technology the laser can deliver pulses of 25 J with a duration of 25 fs per pulse at a repetition rate of 0.1 Hz per pulse and wavelength $\lambda = 800$ nm. In the low power mode the laser can operate at an increased repetition rate of 10 Hz delivering 45 TW per pulse. Two off-axis parabolic mirrors are used for focusing the beam, one with 320 cm focal length and the second with 40 cm, depending on application. While the first one will be used for laser-wakefield acceleration of electrons in a gaseous target the second mirror will be employed for producing protons and ion beams from solid targets.

Concerning acceleration of electrons two types of experiments are planned at CETAL. In order to simulate the radiation belt around the planet Jupiter electron energies up to 100 MeV and with an exponential energy decay in the electron bunch will be produced using a fast gas valve. Acceleration of electrons in a controlled gas pressure of a few torrs will be realized using a dedicated gas cell with variable length. In this respect simulating the experimental conditions is of high interest in order to identify the operating acceleration regimes.

Both experiments and particle-in-cell simulations (PIC) have proven that the use of cones as the targets with which the ultra-high and ultra-short laser pulse interacts goes to the increase of the efficiency to generate proton beams with high kinetic energy [10–12].

In order to prepare experiments on CETAL in which electrons and protons (ions) are accelerated we do PIC simulations for different type of targets, gaseous or solid and different intensities of the ultra-short laser pulses. All the simulations are new, because they are done for the laser parameters, which was not considered in any previous work.

In Section 2 we describe the PIC simulation method and the specific PIC code used, PICLS. The results of the PIC simulations are presented in the Section 3 which has two subsections. The laser wakefield acceleration of the electrons in the bubble regime is obtained in Section 3.1. The proton acceleration in the interaction of the ultra-high intensity laser with solid targets is described in the Section 3.2. We conclude with some remarks and future expectations in Section 4.

2. THEORY

Particle-in-cell simulations model laser-plasma interaction by solving the plasma particles movement and Maxwell's equations when the space occupied by the plasma is partitioned by a mathematical grid. In any program which does PIC simulations at each time step the fields are solved and then the particles are moved. From PIC simulations we can find the velocity of the plasma particles in space, the particle densities, the electric and magnetic fields and the currents of the particles. We used the 2D version of PICLS [13], which is a 3D relativistic Particle-in-Cell code. The simulations were done on the BlueGene supercomputer from the West University of Timisoara and on the server from CELIA, Bordeaux, France. We chose in all simulations a high intensity laser pulse with the wavelength $\lambda_0 = 800$ nm, the period $\tau_0 = 2.66$ fs, the duration $\tau = 25$ fs, and the peak energy 25 J, which corresponds to the ultrahigh laser pulses of the CETAL laser and 1 PW output of ELI-NP HPLS (High Power Laser System). We have worked with a Gaussian laser pulse and linear p-polarized, *i.e.*, $E_y \neq 0$ and $E_z = 0$. The laser pulse comes always from the left side of the target and we have a vacuum before the plasma. The plasma (electron) density n_e was chosen higher than the critical density n_c (overdense plasma) or less than the critical density (underdense plasma). Critical density of the plasma means the density of the plasma for which the plasma frequency is equal with the laser frequency.

3. RESULTS

3.1. ELECTRON ACCELERATION IN THE BUBBLE REGIME

We studied the laser wakefield acceleration of the electrons in the bubble regime at the interaction of the ultra-high power laser pulse with a Helium gas with the density $0.05 n_c$ and the intensity of the laser pulse 10^{22} W/cm². The short Helium gas jet can already be produced [14]. The Helium gas target has the thickness of $111 \mu\text{m}$. The simulation time is 2 ps. The grid step-size in the x direction and in y direction is 80 nm. The time step of the simulation is 0.26 fs. In a grid cell we considered 21 macroparticles. The electron density in space is drawn in Figure 1.

The most energetic electrons and the highest density is obtained in the direction of laser propagation, in the center of so called bubble, as a bunch of electrons. The highest kinetic energy achieved by the electrons is 940 MeV as can be seen in Figure 2. The maximum electron energy in the simulation box starts to decrease when the most energetic electrons exit through the right boundary.

3.2. PROTON ACCELERATION

The interaction of an ultra-short laser pulse with a solid target leads to the protons acceleration by the hot electrons (or Target Normal Sheath Acceleration,

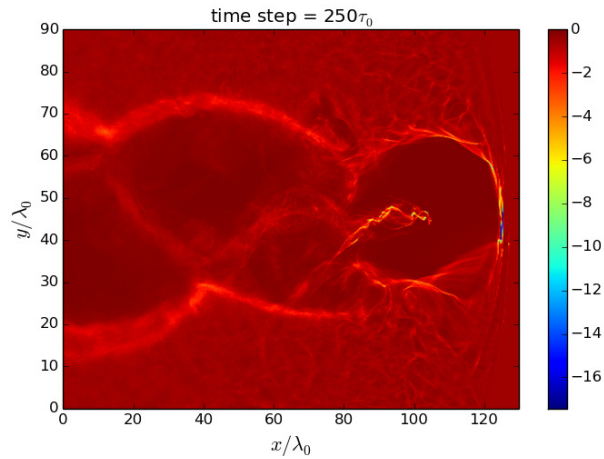


Fig. 1 – The electron density for the interaction of the ultra-high power laser pulse with a Helium gas target with the thickness of $111 \mu\text{m}$ after 665 fs . The x and y axis are in laser wavelengths, λ_0 . The proton density from the right side of the figure is in critical densities (a value of 0.54 for density corresponds at $0.1 n_c$).

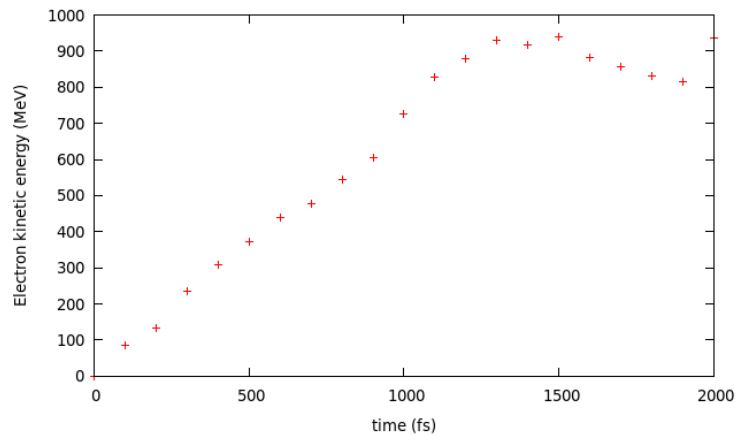


Fig. 2 – The maximum electron kinetic energy for the interaction of the ultra-high power laser pulse with a Helium gas target.

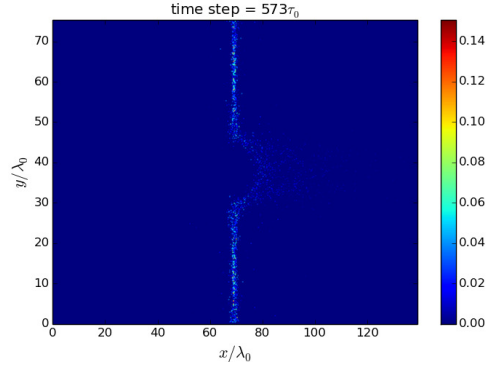


Fig. 3 – The proton density for the interaction of the ultra-high power laser pulse with a foil target with the thickness of $0.2 \mu\text{m}$ after 1.5 ps. The x and y axis are in laser wavelengths, λ_0 . The proton density from the right side of the figure is in critical densities (a value of 0.135 for density corresponds at $300 n_c$).

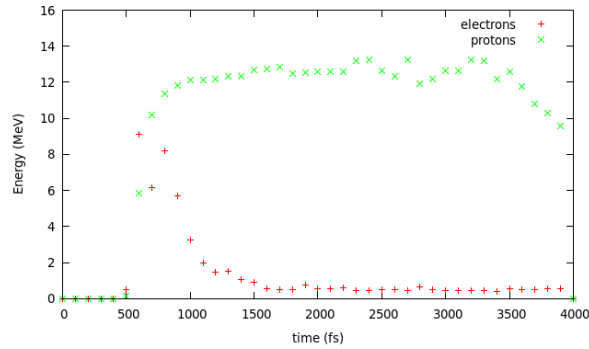


Fig. 4 – The maximum proton kinetic energy for the interaction of the ultra-high power laser pulse with a with a foil target with the thickness of $0.2 \mu\text{m}$.

TNSA). We do two dimensional PIC simulations for a foil target with the thickness of $0.2 \mu\text{m}$, a ultra-high laser pulse with the intensity of 10^{21} W/cm^2 and a time simulation of 4 ps. The grid step-size in both directions, x and y is 12 nm, with 21 macroparticles per cell and the time step is 0.04 fs. In this case the proton density is shown in Figure 3.

We obtained the highest kinetic energy of the protons to be 14 MeV (Figure 4). We simulated also the interaction of the same ultra-high power laser pulse with a flat-top cone targets with curved walls. We considered a cone with the hight of $50 \mu\text{m}$ and the the inner neck of $5 \mu\text{m}$. The flat-top of the cone has a height of $24 \mu\text{m}$ and a thickness of $4 \mu\text{m}$. The plasma density, grid step-size, the macroparticles per cell and the time step are same as in the previous case of the foil target. The proton

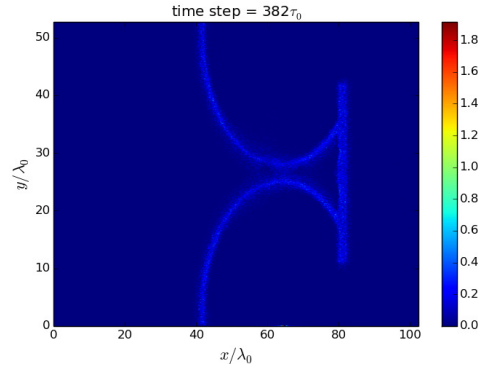


Fig. 5 – The proton density for the interaction of the ultra-high power laser pulse with a flat-top cone target after 1 ps. The x and y axis are in laser wavelengths, λ_0 . The proton density from the right side of the figure is in critical densities (a value of 0.16 for density corresponds at $300 n_c$).

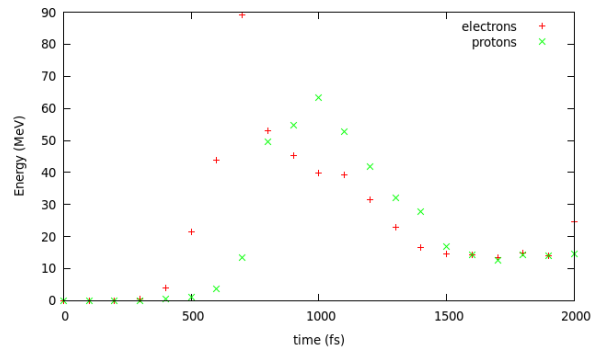


Fig. 6 – The maximum proton kinetic energy for the interaction of the ultra-high power laser pulse with a flat-top cone target with the thickness of the flat-top μm .

density after 1 ps from the beginning of the simulation is plotted in Figure 5.

The highest kinetic energy achieved by the protons is 70 MeV as can be seen in Figure 6.

We can see from figures 4 and 6 that the energy transfer from electrons to protons occurs on longer timescale in the case of the cone. We also computed laser absorption for the foil and cone targets. In the case of the cone target the laser absorption is 10%, but for the foil target the laser absorption is almost 2%. The cone target is more efficient in the absorption of the laser energy.

4. CONCLUSIONS

We studied the electron and proton acceleration in the interaction of ultra-high power laser pulses with gaseous and foil and cone targets. For the LWFA electron acceleration we obtained energies about 1 GeV. The cone target is better than the foil target to obtain colimated beam of accelerated protons with a high power laser. In the future work, in order to increase the kinetic energy of the electrons for lower intensities, we must decrease the density of the gas target. The interaction of a laser pulse with a very high intensity laser will accelerate electrons at kinetic energies of GeV order. We will improve the dimensions of the cone target to get colimated beams of protons with kinetic energies of order of hundreds MeV.

Acknowledgements. This research received funding from ELI-NP. The ELI-NP project is co-funded by The European Union through the European Regional Development Fund. CMT and OB are funded by the Institute of Atomic Physics (IFA) within the CERN-RO program, specialty ELI-NP, through contract LAPLACE E06.

REFERENCES

1. T. Tajima and J. M. Dawson, *Phys. Rev. Lett* **43**, 267 (1979).
2. W. P. Leemans, A. J. Gonsalves, H.-S. Mao, K. Nakamura, C. Benedetti, C. B. Schroeder, Cs. Tóth, J. Daniels, D. E. Mittelberger, S. S. Bulanov, J.-L. Vay, C. G. R. Geddes, and E. Esarey, *Phys. Rev. Lett.* **113**, 245002 (2014).
3. Xiaoming Wang, Rafal Zgadzaj, Neil Fazel, Zhengyan Li, S. A. Yi, Xi Zhang, Watson Henderson, Y.-Y. Chang, R. Korzekwa, H.-E. Tsai, C.-H. Pai, H. Quevedo, G. Dyer, E. Gaul, M. Martinez, A. C. Bernstein, T. Borger, M. Spinks, M. Donovan, V. Khudik, G. Shvets, T. Ditmire, and M. C. Downer, *Nature Communications* **4**, 1988 (2014).
4. H. T. Kim, K. H. Pae, H. J. Cha, I Jong Kim, T. J. Yu, J. H. Sung, S. K. Lee, T. M. Jeong, and J. Lee, *Phys. Rev. Lett.* **111**, 165002 (2013).
5. M. Hegelich, S. Karsch, G. Pretzler, D. Habs, K. Witte, W. Guenther, M. Allen, A. Blazevic, J. Fuchs, J.C. Gauthier, M. Geissel, P. Audebert, T. Cowan, and M. Roth, *Phys. Rev. Lett.* **89**, 085002 (2002).
6. A. Pukhov and J. Meyer-ter-Vehn, *Appl. Phys. B* **74**, 355 (2002).
7. A. Maksimchuk, S. Gu, K. Flippo, V. Y. Bychenkov, and D. Umstadter, *Phys. Rev. Lett.* **84**, 4108 (2000).
8. S. P. Hatchett *et al.*, *Phys. Plasmas* **7**, 2076 (2000).
9. E. L. Clark *et al.*, *Phys. Rev. Lett.* **87**, 670 (2000).
10. K. A. Flippo *et al.*, *Phys. Plasmas* **15**, 056709 (2008).
11. N. Renard-Le Galloudec, and E. d'Humières, *Laser Part. Beams* **28**, 513 (2010).
12. E. d'Humières, A. Brantov, V. Yu. Bychenkov, and V. T. Tikhonchuk, *Phys. Plasmas* **20**, 023103 (2013).
13. Y. Sentoku and A. Kemp, *J. Comput. Phys.* **227**, 6846 (2008).
14. F. Sylla, M. Veltcheva, S. Kahaly, A. Flacco, and V. Malka, *Rev. Sci. Instrum.* **83**, 033507 (2012).